European Journal of Medicinal Chemistry 74 (2014) 477–490

Contents lists available at ScienceDirect

European Journal of Medicinal Chemistry

journal homepage: http://www.elsevier.com/locate/ejmech

Short communication

Synthesis, docking and pharmacological evaluation of novel indole based potential atypical antipsychotics

Alka Bali*, Umesh Sen, Tania Peshin

University Institute of Pharmaceutical Sciences, UGC Center of Advanced Study, Panjab University, Chandigarh, 160014, India

ARTICLE INFO

Article history:
Received 17 May 2013
Received in revised form
9 September 2013
Accepted 11 September 2013
Available online 21 September 2013

Keywords:
Atypical antipsychotics
Indole derivatives
Log BB
D_2/5-HT_{2A} antagonists
In silico
Docking studies

ABSTRACT

A series of substituted indole derivatives have been synthesized and the target compounds evaluated for atypical antipsychotic activity in apomorphine induced mesh climbing and stereotypy assays in mice. The compounds **11** and **12** have emerged as important lead compounds showing potential atypical antipsychotic profile. *In silico* (docking studies) have been carried out to postulate a hypothetical binding model for the target compounds with respect to the dopaminergic D_2 and 5-HT_{2A} receptors. Theoretical ADME profiling of the compounds based on selected physicochemical parameters has suggested an excellent compliance with Lipinski's rules. The potential of these compounds to penetrate the blood brain barrier (log BB) was computed through an online software program and the values obtained for the compounds suggest good potential for brain permeation.

1. Introduction

Schizophrenia is a chronic, debilitating mental disorder striking 1–2% of the global population with a median lifetime prevalence of 0.7–0.8%, and is associated with mortality rates 2–3 times higher than those in the general population [1,2]. After nearly a century of research, the exact etiology and pathophysiology of schizophrenia remain largely unresolved. The most widely considered neurochemical hypothesis of schizophrenia, that is, the dopaminergic hypothesis postulates increased dopamine release and sensitization of the dopaminergic system as the major causes of schizophrenic manifestations [3] and most approved antipsychotics target dopamine receptors. The classical or 'typical' neuroleptics (first generation antipsychotics) such as chlorpromazine, haloperidol, fluphenazine have been postulated to alleviate the active or positive symptoms of the disease through inhibition of the postsynaptic dopaminergic transmission in mesolimbic areas of brain associated with integration of emotions and behavior [4]. However, their actions in the nigrostriatal regions of the brain associated with locomotor coordination results in severe mechanism related side effects including parkinsonism and akathesia (extrapyramidal symptoms), tardive dyskinesia and galactorrhea (due to increased prolactin release) [5,6]. Moreover, these compounds are ineffective against the negative symptoms of schizophrenia. Approximately 30% of patients do not respond to typical antipsychotics and EPS can become a treatment-limiting side effect. Second generation agents such as the prototypic agent clozapine, possess lower affinity for dopamine D_2 receptors. The atypical antipsychotic profile of clozapine is thought to result from its affinity for a multitude of receptors, including dopamine receptor subtypes, 5-HT_2 receptors, and α_1 adrenoceptors [7]. This multiple receptor effect also accounts for several adverse effects involving metabolic disturbances leading to increase in body weight, diabetes, changes in mood, sexual dysfunction, and agranulocytosis [8] which considerably restrain the therapeutic applicability of this drug. In the recent years, several diverse receptor binding approaches have emerged for the design of newer atypical antipsychotics. Some dopaminergic and serotonergic approaches seem really promising, e.g., selective affinity for D_4 or D_3 receptors (*versus* D_2 receptors) [9,10] and combined D_2/5-HT_2 affinity [11,12]. Several other approaches are there still at investigational level [13–15]. However, none of these can exclusively account for the existence of atypical profile in atypical antipsychotics currently in use, e.g., risperidone, ziprasidone, clozapine and others. This fact is particularly corroborated by the recent literature reports highlighting the multireceptor targetting approaches being pursued in this area [16–19]. In animal

* Corresponding author. Tel.: +91 172 2541142; fax: +91 172 541142.
E-mail addresses: alka.bali@rediffmail.com, alkaa.bali@gmail.com (A. Bali).

0223-5234/$ – see front matter © 2013 Elsevier Masson SAS. All rights reserved.
http://dx.doi.org/10.1016/j.ejmech.2013.09.020

models, it is widely accepted that atypical antipsychotics can be identified by their inhibition of apomorphine induced climbing response (indicative of action in mesocorticolimbic region; antipsychotic effect) along with weak or no inhibition of apomorphine induced stereotypy (indicative of sparing the nigrostriatal system; reduced extrapyramidal side effect liability) [20].

We had recently reported series of substituted aryl piperazines [21–23] with some of the lead molecules displaying good atypical antipsychotic profiles. In our present paper, we report the synthesis, pharmacological evaluation and docking studies on a novel series of indole based non-piperazine derivatives which incorporate a phenoxy system as a replacement for the piperazine system (Fig. 1). *In silico* (docking studies) were done to investigate the hypothetical binding mode of the target compounds to the dopaminergic D_2 receptors and the serotonergic 5-HT_{2A} receptors. A binding model has been proposed based on the docking studies. Since, the compounds were intended to be CNS active, their potential to cross the blood brain barrier was computed through an online software program in terms of their log BB values.

2. Results and discussion

2.1. Synthesis of compounds

Table 1 shows the chemical structures of the synthesized compounds. Synthetic scheme for preparation of target compounds is summarized in Fig. 2. The synthetic procedure primarily involved the synthesis of phenyl hydrazones followed by cyclization of the phenyl hydrazones to obtain indole derivatives (Fischer indole synthesis) [24], synthesis of chloropropyl aniline derivatives and the final coupling of indole and chloropropyl aniline derivatives to yield the target compounds.

In the first step, phenylhydrazine was reacted with para- or ortho-hydroxy acetophenones in equimolar proportions in presence of few drops of acid catalyst glacial acetic acid and ethanol to form the corresponding acetophenone phenylhydrazones (**1**–**2**) in very good yields ranging from 90 to 95%. These were further cyclized by heating in polyphosphoric acid to form 4- and 2- (1*H*-indol-2-yl) substituted phenols **3**–**4** respectively in yields more than 80%. Further, para and ortho chloroanilines and para- and ortho-anisidines were separately refluxed with 1-bromo-3-chloropropane in equimolar amounts in presence of ethyl methyl ketone affording the 4- and 2-chloro-*N*-(3-chloropropyl)phenylamines (**5**–**6**) and *N*-(3-chloropropyl) substituted 4- and 2-methoxyphenylamines (**7**–**8**) respectively in yields ranging from 68 to 77%. Similar yields were also obtainable using acetone as a solvent instead of ethyl methyl ketone. The use of ethyl methyl ketone, however, offered the advantage of much shorter reaction time as a 24 h reaction in acetone was found to be complete in 8 h in ethyl methyl ketone. The final compounds **9**–**14** were synthesized by heating equimolar proportions of the 1*H*-indol-2-yl-phenols (**3**–**4**) and the chloropropyl aniline derivatives (**5**–**8**) at a temperature of 70–80 °C in acetone in the presence of twice molar amounts of potassium carbonate. Final compounds were obtained in reasonably good yields (62–68%). All the reactions were monitored by thin layer chromatography and the final products were characterized through UV, NMR, IR and mass spectroscopic data.

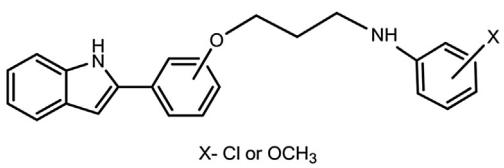

Fig. 1. General structure of the test compounds.

Table 1
Pharmacological evaluation for atypical antipsychotic profile.

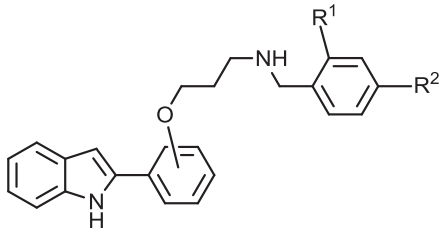

Compound	R^1	R^2	O-Pr	Reversal of apomorphine induced mesh climbing[a]	Reversal of apomorphine induced stereotypy[a]	ED_{50} (mg/kg) (mesh climbing)[b]
9	H	Cl	o-	+	−	7.23 ± 0.27
10	Cl	H	o-	+	−	6.23 ± 0.23
11	H	Cl	p-	+	−	1.80 ± 0.09
12	Cl	H	p-	+	−	1.60 ± 0.07
13	H	OCH_3	p-	+	+	1.90 ± 0.29
14	OCH_3	H	p-	+	+	1.70 ± 0.06
Clozapine	–	–	–	+	−	3.07 ± 0.12

[a] Statistically significant reduction compared to control at $p < 0.05$ (One way ANOVA followed by Tukey test).
[b] Calculated from results for antipsychotic activity (mesh climbing assay) at three graded doses ($n = 5$).

2.2. Preliminary pharmacological evaluation for atypical antipsychotic effect

The prepared target compounds **9**–**14** were evaluated for atypical antipsychotic effect by *in vivo* pharmacological evaluation studies. In animal models, the inhibition of apomorphine induced mesh climbing response signifies dopaminergic antagonism in mesocorticolimbic pathway indicative of potential antipsychotic effect. Further, an inhibition of apomorphine induced stereotypy is characteristic of antagonism in the nigrostriatal system linked to the propensity to cause extrapyramidal symptoms [20]. Prior permission of the Institutional Animal Ethics Committee (IAEC) was obtained and all experiments were conducted according to the approved protocol. All the animals were allowed free access to food and water (*ad libidum*), in a constant light–dark cycle. The general behavior of the animals was normal during the course of the experiment. Doses were selected by initial titration at different dose levels. Clozapine group was employed as a standard (positive control). Statistical comparison of the results obtained in the test groups with control and standard groups was carried out using one way ANOVA ($p < 0.01$) (Jandel Sigmastat version 2.0) followed by TUKEY test fixing the significance level at $p < 0.05$.

The ED_{50} values for test compounds and standard drug (clozapine) are reported in Table 1. Mean score for all the test compounds and clozapine in both the assays is tabulated in Table 2 and graphically depicted in Fig. 3. The test compounds **9**–**14** produced statistically significant reversal of apomorphine induced mesh climbing indicating potential antipsychotic effect. Amongst these, **9**–**12** did not produce statistically significant reduction in the stereotypy assay suggesting an atypical profile. However, the compounds **13** and **14** also reversed apomorphine induced stereotypy signifying that these are also acting in nigrostriatal regions of the brain and hence, do not possess an atypical antipsychotic profile.

All compounds have demonstrated very good efficacy in the mesh climbing assay with ED_{50} values ranging from 1.70 to 7.23

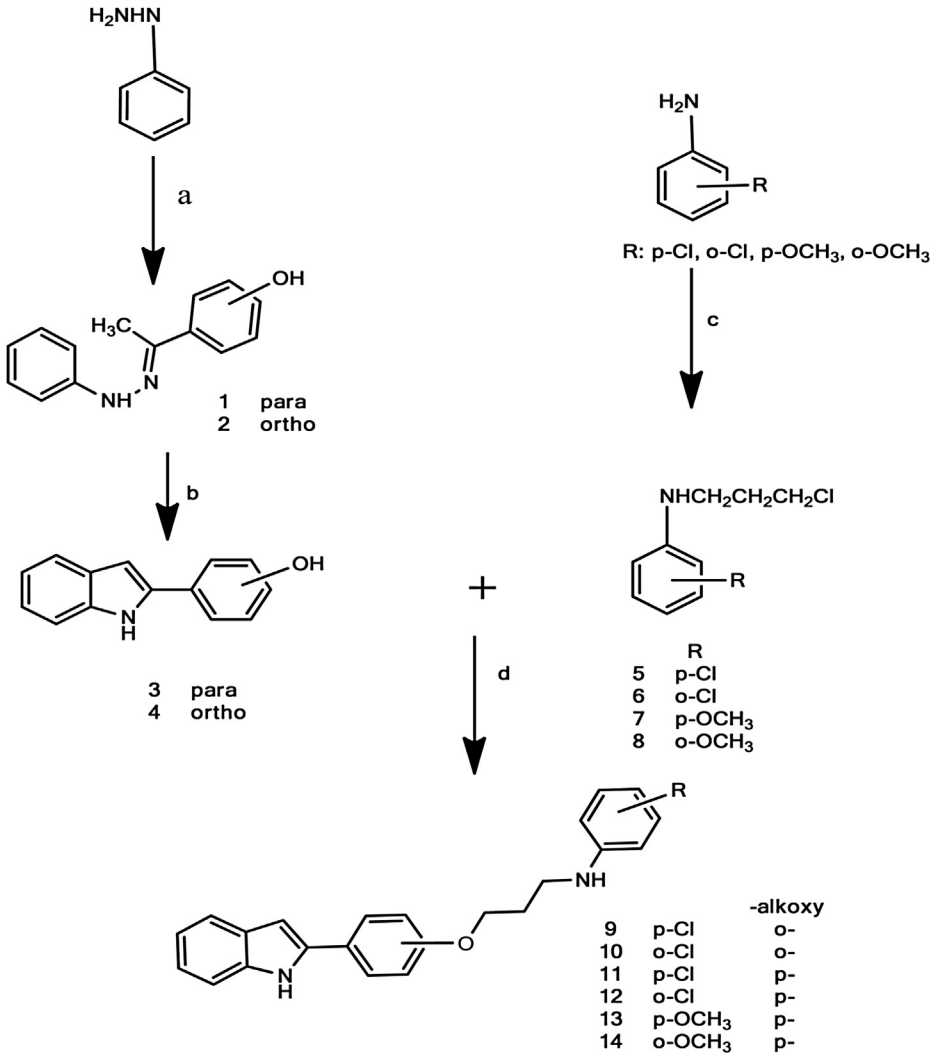

Fig. 2. Synthetic scheme for the preparation of the test compounds.

(clozapine; 3.07). However, the compounds with ortho indole substitution on the phenoxy ring **11** and **12** have shown a relatively higher potency compared to their para analogs **9** and **10** respectively. As evident from the ED_{50} values, all para substituted analogs, **11** to **14** have shown greater antipsychotic effect compared to the standard drug clozapine. However, amongst these, the methoxy analogs **13** and **14** do not seem to exhibit an atypical profile. Further, the compounds **11** and **12** were found to cause a reversal in stereotypy at doses higher than 5 mg/kg. However, considering their effective doses in mesh climbing assay (for antipsychotic effect), these can still be considered as potential atypical antipsychotics.

2.3. *In silico evaluation and computational studies*

2.3.1. *In silico (docking) studies*

Docking (*in silico*) studies were performed on the compounds **9**–**14** found active in the mesh climbing assay in order to postulate a hypothetical binding model for their interaction with 5-HT_{2A} and D_2 receptors. Reference drugs (ziprasidone, ketanserin and eticlopride) known to possess affinity for 5-HT_{2A} and D_2 receptors were also included in the docking studies for comparison. Table 3 shows the glide docking scores obtained for the various test compounds and the reference with respect to 5-HT_{2A} and D_2 receptors. Figs. 4 and 5 show the ligand interaction diagrams for the test compounds with 5-HT_{2A} and D_2 receptors respectively. Figs. 6 and 7 show the hypothetical binding modes for the reference drugs and test compounds **11** and **12** within the 5-HT_{2A} and D_2 receptor pockets.

2.3.1.1. 5-HT_{2A} receptor docking. Currently, there is no crystal structure of the 5-HT_{2A} receptor lodged in the Protein Data bank (PDB), hence, the model employed for the *in silico* evaluation was retrieved from (Uniprot ID: P28233) [25]. Amongst the standard drugs, ketanserine bound best to the 5-HT_{2A} receptor affording highest dock score. The charged piperazine NH was involved in a strong charge reinforced hydrogen bond (1.909 Å) with the carboxylate oxygen of the conserved residue Asp155. Another strong hydrogen bond was observed between the carbonyl oxygen of dihydropyridinedione moiety and indole NH of Trp151 residue (1.799 Å). Hydrophobic interactions of fluorine atom with Phe125 and Val130 and van der Waals interactions with proximately located residues Pro129, Leu126, Leu154, Phe158, Val204 and Met208 within a distance range of 3 Å further strengthened the receptor ligand bonding. Risperidone also showed similar hydrogen bonds with Asp155 (piperazine NH) and Trp151 (with tetrahydropyridopyrimidinone system) residues. Strong van der Waals interactions were seen with residues Leu126, Val130, Ile152,

Table 2
Mean score in apomorphine induced mesh climbing and stereotypy assays.

Treatment	Average score at time (min)									
	10		15		20		25		30	
	C	St	C	St	C	St	C	St	C	St
Naïve Group	6.5 ± 0.29[a]	5.3 ± 0.25[a]	6.0 ± 0.29[a]	5.5 ± 0.29[a]	5.5 ± 0.29[a]	5.3 ± 0.25[a]	5.5 ± 0.29[a]	4.8 ± 0.48[a]	4.8 ± 0.25[a]	4.8 ± 0.48[a]
Control (2.5 mg/kg)	13.0 ± 1.72	8.3 ± 0.25	18.8 ± 0.75	8.3 ± 0.48	17.5 ± 0.24	8.8 ± 0.48	17.3 ± 1.49	8.8 ± 0.85	15.0 ± 0.63	7.3 ± 0.25
Clozapine (2.5 mg/kg)	8.3±0.25[a]	8.5 ± 0.29	7.8 ± 0.48[a]	8.8 ± 0.25	6.5 ± 0.29[a]	8.3 ± 0.25	6.5 ± 0.29[a]	8.8 ± 0.25	6.8 ± 0.25[a]	8.0 ± 0.00
Clozapine (5 mg/kg)	6.3±0.25[a]	8.5 ± 0.29[a]	6.3±0.25[a]	8.3 ± 0.25[a]	6.0 ± 0.41[a]	8.3 ± 0.25[a]	5.8 ± 0.25[a]	8.0 ± 0.00[a]	5.8 ± 0.258[a]	7.8 ± 0.48[a]
9 (5 mg/kg)	7.6 ± 0.24[a]	7.6 ± 0.24[a]	8.2 ± 0.37[a]	7.4 ± 0.24[a]	7.4 ± 0.24[a]	7.6 ± 0.24[a]	7.6 ± 0.24[a]	7.2 ± 0.20[a]	6.8 ± 0.20[a]	7.0 ± 0.44[a]
9 (7.5 mg/kg)	7.4 ± 0.24[a]	8.2 ± 0.20	7.2 ± 0.37[a]	7.8 ± 0.37	6.4 ± 0.24[a]	8.0 ± 0.00	6.4 ± 0.24[a]	7.2 ± 0.20	5.6 ± 0.24[a]	7.0 ± 0.44
9 (10 mg/kg)	6.2 ± 0.37[a]	8.6 ± 0.24	5.6 ± 0.40[a]	8.0 ± 0.32	5.6 ± 0.51[a]	7.8 ± 0.20	5.0 ± 0.31[a]	7.4 ± 0.24	4.4 ± 0.40[a]	6.8 ± 0.49
10 (5 mg/kg)	7.4 ± 0.25[a]	8.2 ± 0.38	7.0 ± 0.31[a]	8.0 ± 0.54	6.6 ± 0.24[a]	8.4 ± 0.40	6.6 ± 0.25[a]	8.4 ± 0.25	6.6 ± 0.25[a]	7.8 ± 0.38
10 (7.5 mg/kg)	6.8 ± 0.38[a]	8.4 ± 0.25	6.6 ± 0.24[a]	7.8 ± 0.38	6.6 ± 0.25[a]	7.8 ± 0.38	6.0 ± 0.31[a]	7.8 ± 0.20	4.6 ± 0.40[a]	7.2 ± 0.38
10 (10 mg/kg)	5.4 ± 0.40[a]	7.8 ± 0.37	5.0 ± 0.45[a]	7.6 ± 0.40	5.2 ± 0.49[a]	7.6 ± 0.4	4.4 ± 0.24[a]	8.0 ± 0.32	3.8 ± 0.20[a]	7.4 ± 0.24
11 (2 mg/kg)	8.8 ± 0.25[a]	8.3 ± 0.25	8.3 ± 0.48[a]	8.0 ± 0.41	8.3 ± 0.25[a]	7.8 ± 0.25	8.0 ± 0.41[a]	7.8 ± 0.25	7.5 ± 0.29[a]	7.0 ± 0.0
11 (5 mg/kg)	8.0 ± 0.41[a]	7.8 ± 0.25[a]	7.8 ± 0.48[a]	7.5 ± 0.29[a]	7.8 ± 0.25[a]	7.0 ± 0.41[a]	7.5 ± 0.29[a]	6.8 ± 0.25[a]	7.5 ± 0.5[a]	7.0 ± 0.41[a]
11 (7.5 mg/kg)	7.5 ± 0.29[a]	7.5 ± 0.29[a]	6.8 ± 0.25[a]	6.8 ± 0.25[a]	6.5 ± 0.29[a]	6.5 ± 0.29[a]	6.5 ± 0.29[a]	6.8 ± 0.48[a]	6.3 ± 0.25[a]	6.5 ± 0.29[a]
12 (2 mg/kg)	8.5 ± 0.29[a]	8.0 ± 0.0	8.3 ± 0.25[a]	8.3 ± 0.25	8.0 ± 0.41[a]	7.8 ± 0.25	7.8 ± 0.25[a]	7.5 ± 0.29	7.5 ± 0.29[a]	7.3 ± 0.48
12 (5 mg/kg)	7.8 ± 0.25[a]	7.5 ± 0.29[a]	7.8 ± 0.25[a]	7.5 ± 0.29[a]	7.5 ± 0.29[a]	7.0 ± 0.41[a]	7.3 ± 0.25[a]	6.8 ± 0.25[a]	7.0 ± 0.41[a]	7.0 ± 0.0[a]
12 (7.5 mg/kg)	7.3 ± 0.25[a]	7.3 ± 0.25[a]	7.0 ± 0.41[a]	6.8 ± 0.25[a]	6.3 ± 0.25[a]	6.5 ± 0.29[a]	6.3 ± 0.25[a]	6.8 ± 0.25[a]	6.4 ± 0.25[a]	6.3 ± 0.25[a]
13 (2.5 mg/kg)	8.8 ± 0.25[a]	7.8 ± 0.25[a]	8.8 ± 0.25[a]	7.8 ± 0.25[a]	8.0 ± 0.41[a]	7.8 ± 0.25[a]	8.3 ± 0.25[a]	7.3 ± 0.25[a]	7.5 ± 0.29[a]	7.0 ± 0.41[a]
13 (5 mg/kg)	7.8 ± 0.25[a]	7.3 ± 0.25[a]	7.8 ± 0.25[a]	6.8 ± 0.25[a]	7.0 ± 0.41[a]	6.8 ± 0.25[a]	5.8 ± 0.25[a]	6.5 ± 0.29[a]	5.5 ± 0.29[a]	7.0 ± 0.44[a]
13 (7.5 mg/kg)	7.5 ± 0.29[a]	6.8 ± 0.25[a]	7.0 ± 0.0[a]	6.0 ± 0.0[a]	7.0 ± 0.41[a]	5.5 ± 0.29[a]	6.5 ± 0.29[a]	5.5 ± 0.29[a]	6.3 ± 0.25[a]	4.5 ± 0.29[a]
14 (2.5 mg/kg)	8.5 ± 0.29[a]	7.3 ± 0.25[a]	8.3 ± 0.25[a]	7.3 ± 0.25[a]	7.5 ± 0.29[a]	6.8 ± 0.25[a]	7.0 ± 0.41[a]	6.5 ± 0.29[a]	6.8 ± 0.25[a]	6.5 ± 0.29[a]
14 (5 mg/kg)	7.5 ± 0.29[a]	6.3 ± 0.25[a]	7.5 ± 0.29[a]	6.3 ± 0.25[a]	7.3 ± 0.25[a]	5.8 ± 0.25[a]	6.8 ± 0.25[a]	5.3 ± 0.48[a]	6.5 ± 0.29[a]	5.0 ± 0.41[a]
14 (7.5 mg/kg)	7.0 ± 0.0	5.5 ± 0.29[a]	6.8 ± 0.25[a]	5.8 ± 0.25[a]	6.5 ± 0.29[a]	5.3 ± 0.25[a]	6.3 ± 0.25[a]	5.0 ± 0.41[a]	6.3 ± 0.25[a]	5.5 ± 0.86[a]

All values are expressed as mean ± S.E.M. ($n = 5$).
C: Apomorphine Induced mesh climbing.
St: Apomorphine Induced stereotypy.
[a] Significantly different from control at $P < 0.05$; One way ANOVA followed by Tukey test.

Leu154, Phe158 and Met208 within 2.5 Å distance. In case of ziprasidone, no interaction was seen with the conserved residue Asp155. However, hydrogen bonding interaction with the indole NH of Trp151 residue was present. Further, at a ring to ring distance of 3.522 Å, a strong π–π stacking was observed between the benzene ring of indolinone moiety and the phenyl ring of Phe158 residue. The exposed chloro group showed hydrophobic interactions with Leu122, Leu126, Phe158 and additional van der Waals interactions were noted with Ile118, Phe193, Ile196, Ile197 and Trp200.

In case of the test compounds, hydrogen bonding interactions with the conserved residue Asp155 were seen with the compounds **12**, **13** and **14**. The compounds **9** and **10** showed somewhat similar docking behavior with absence of any hydrogen bonding interaction. However, the chlorophenyl and phenoxy rings in both the compounds showed π–π stacking with phenyl ring of Phe158 and indole group of Trp200 accounting for their decent dock scores. The chloro group was involved in hydrophobic interactions with Leu154, Val204 and Met208. The para chloro group was found interacting hydrophobically with Leu154, Val204 and Met208 at

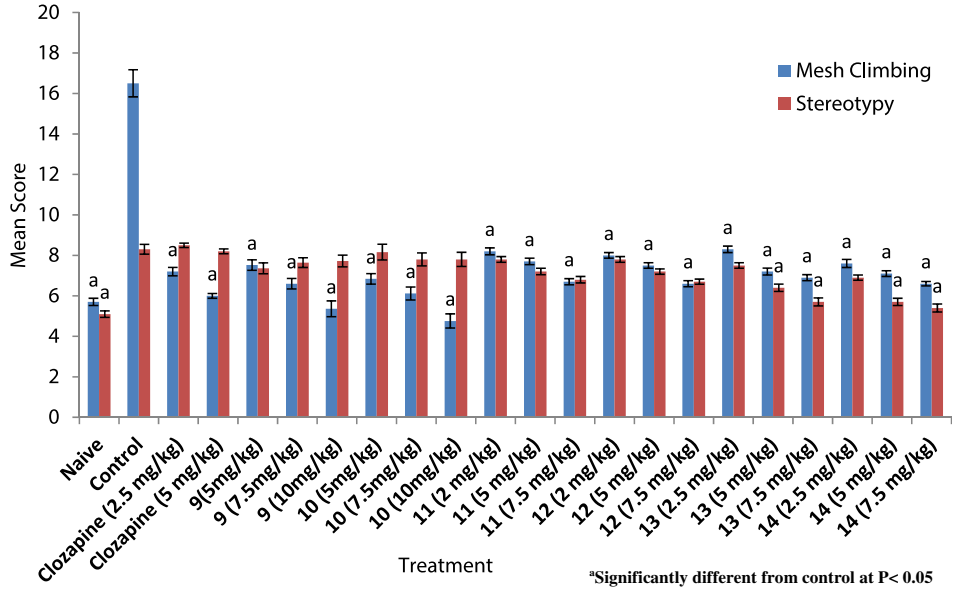

Fig. 3. Mean score (mean time) in apomorphine induced mesh climbing and stereotypy assays.

Table 3
DockScore of the active compounds.

Compound no.	Glide Dock score (5-HT_{2A})	Rank score (5-HT_{2A})	Glide Dock score (D_2)	Rank score (D_2)
9	−3.459	4	−7.376	2
10	−2.990	5	−7.420	1
11	−6.256	1	−6.802	3
12	−2.711	6	−6.433	4
13	−4.237	3	−4.232	6
14	−4.944	2	−5.939	5
Ziprasidone	−3.904	Standard	−8.096	Standard
Ketanserin	−4.188	Standard	−3.471	Standard
Risperidone	−3.306	Standard	−7.387	Standard

respective distances of 3.532, 3.413, 2.613 Å. Additionally, significant van der Waals interactions were seen with the amino acid residues Ile118, Leu122, Leu126, Trp151, Asp155, Ile197 and Thr201 for both the drugs.

The compound **11** showed very good dock score (−6.8023) despite the absence of interaction with Asp155. The phenylamine NH was involved in three hydrogen bonding interactions with Leu362 (3.016 Å), Asn363 (3.287 Å) and Asn363 (3.348 Å) residues. A π−π ring stacking was observed between the chlorophenyl ring and the phenyl moiety of amino acid Phe339. The exposed chloro group showed hydrophobic interactions with residues Thr342 and Asn343 and van der Waals interactions were noted with the

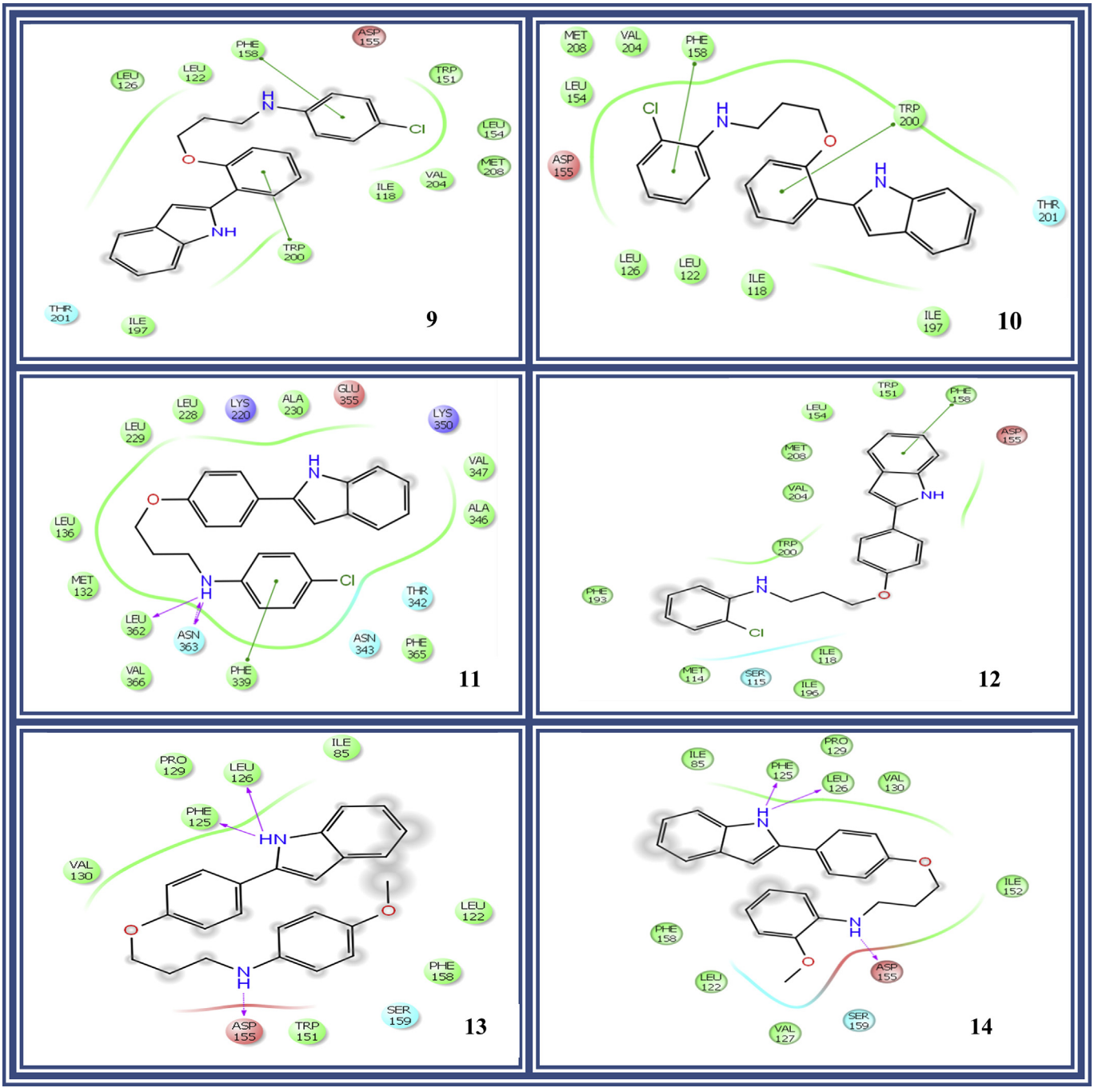

Fig. 4. Ligand interaction diagrams for the test compounds (**9**–**14**) with 5-HT_{2A} receptor.

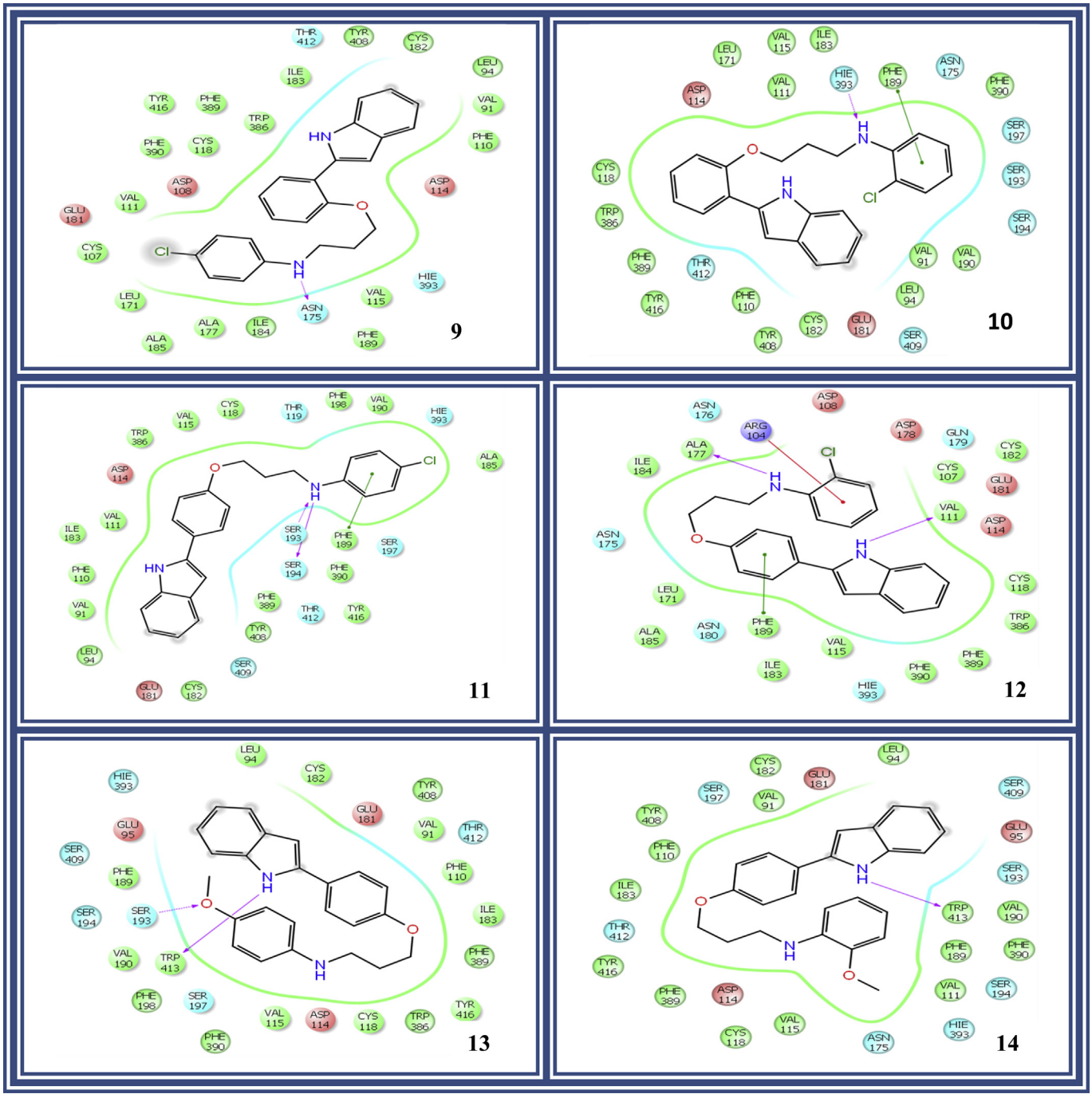

Fig. 5. Ligand interaction diagrams for the test compounds (**9**–**14**) with D_2 receptor.

proximate residues including Leu136, Ala230, Phe339, Asn343, Ala346, Val347, Glu355 and Val366.

Compounds **12**, **13** and **14** displayed quite similar binding profile towards the 5-HT_{2A} receptor. Besides the presence of hydrogen bonding interaction with charged Asp155 in all of these, the indole NH formed two backbone hydrogen bonds with residues Phe125 and Phe126. The indole moiety of the compound **12** additionally showed a π−π stacking with the phenyl ring of Phe158 which were also seen with the compounds **9** and **10**. Hydrophobic interactions were seen with the ortho chloro moiety in **12** with Ile118, Ile196 and Trp200. Similar hydrophobic interactions were also seen for the methoxy groups in compounds **13** and **14** with Leu122 and Phe158.

2.3.1.2. D_2 receptor docking. Currently, there is no crystal structure of the D_2 receptor lodged in the Protein Data bank (PDB), hence, the model employed for the *in silico* evaluation was obtained from ModBase (Uniprot ID: P14416) [26]. Some standard drugs known to possess a good D_2 receptor affinity (ziprasidone and eticlopride) and a weak D_2 receptor affinity (ketanserin) were taken to assess the ability of the model to reproduce their binding profiles. As anticipated, ziprasidone showed good interactions with D_2 receptor. The charged piperazine NH of the drug was involved in a strong charge reinforced hydrogen bonding interaction (1.561 Å) with the conserved residue Asp114. Additionally, both benzene and thiazole rings of benzothiazole moiety were found stacked (π−π stacking) against the phenyl ring of Phe390 at distances of 3.778 and 3.268 Å

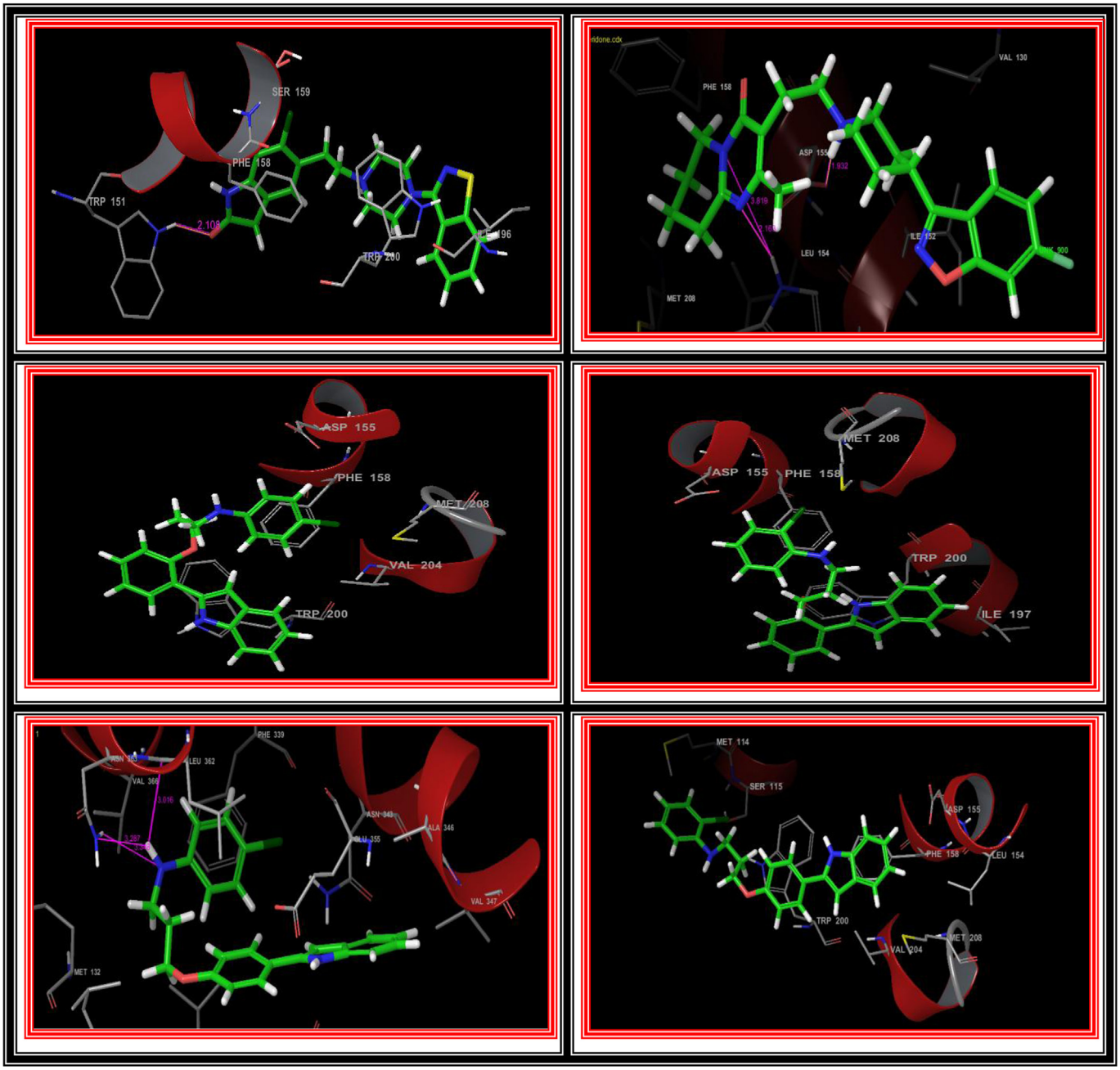

Fig. 6. Docking of Ziprasidone, Risperidone, **9**, **10**, **11**, **12** (row wise left to right) with 5-HT_{2A} receptor.

respectively. The chloro group interacted hydrophobically with Val91 and Phe110 and van der Waals interactions were noted with several amino acids in vicinity as Val115, Cys118, Ile183, Phe189, Ser 193, Ser194, Ser197, Trp386, Phe389, Tyr408, Ser409, Thr412 and Tyr416. Risperidone also showed a charge reinforced hydrogen bond (1.630 Å) with the side chain of amino acid Asp114. Another hydrogen bond was seen between the lactam oxygen and O–H of Thr412. Prominent π–π stackings were also seen with the phenyl ring of benzoxazole moiety stacking well with the phenyl of Phe189 and imidazole rings of His393 and the oxazole ring stacking with the phenyl ring of Phe389. Hydrophobic interactions of the fluoro substituent with Val190 and Ser193 and strong van der Waals interactions with proximately located residues Val91, Phe110, Val111 Val115, Cys118, Ile 183, Val190, Ser 194, Trp386, Phe390, Tyr408, Ser409 and Tyr416 made additional contributions to the drug–receptor complex.

Ketanserine, as expected, showed the least affinity for the receptor. The oxygen atom of the carbonyl linker was involved in a back bone hydrogen bond (2.482 Å) with the amide NH of Ile183 and another hydrogen bond (3.626 Å) was seen between the lactam NH and oxygen atom of Gly98. The fluoro group accounted for some hydrophobic interactions with Val91, Phe110 and Tyr416.

Among the test ligands, compound **9** showed a good docking profile. The phenylamine NH hydrogen of the molecule was involved in a strong hydrogen bond (1.927 Å) with the carbonyl oxygen of Asn175. Strong hydrophobic interactions were noted between the chloro moiety and the residues Cys107, Asp108 and Glu181. The docking model showed very strong van der Waals

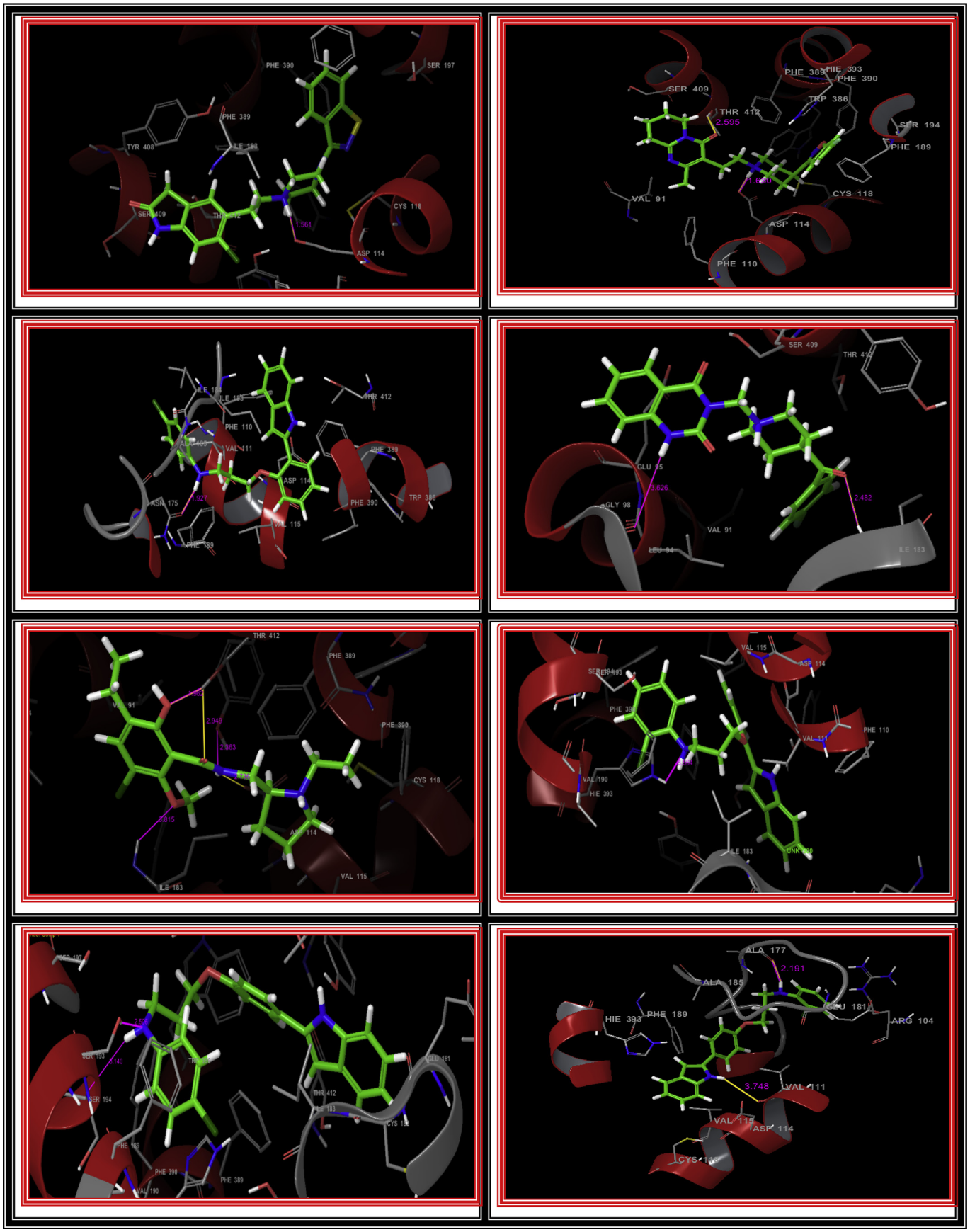

Fig. 7. Docking of Ziprasidone, Risperidone, Ketanserin, Eticlopride, **9**, **10**, **11**, **12** (row wise left to right) with D_2 receptor.

Table 4
Calculation of various molecular properties of target compounds.

Compound	Molecular weight (MW)	Molar refractivity (MR) cm^3/mole	Connolly solvent accessible surface area ($Å^2$)	Connolly molecular surface area ($Å^2$)	Connolly solvent excluded volume ($Å^3$)	Ovality	Log *P*	Log *BB*	Topological polar surface area (TPSA) ($Å^2$)	Molecular topological Index (MTI)	Wiener Index (WI)	No. of H-bond acceptors	No. of H-bond donor NH	no. of violations LR[a]
9	376.87	112.570	586.28	334.76	328.32	1.454	5.133	0.43	29.66	16607	2207	1	2	1
10	376.87	112.570	585.68	333.67	327.44	1.452	5.133	0.50	29.66	16415	2167	1	2	1
11	376.87	112.57	674.64	353.22	299.20	1.632	5.13	0.70	33.29	18203	2423	1	2	1
12	376.87	112.57	666.76	350.83	298.99	1.622	5.13	0.46	33.29	18011	2383	1	2	1
13	372.45	114.23	698.73	366.45	310.27	1.653	4.445	0.38	42.52	20767	2715	2	2	0
14	372.45	114.23	686.83	362.99	310.77	1.635	4.445	0.48	42.52	20223	2635	2	2	0
Clozapine	326.82	95.22	534.29	284.76	262.33	1.436	3.707	0.75	30.87	8127	1082	3	1	0
Ketanserine	381.40	101.58	611.77	326.07	303.63	1.492	2.662	0.89	69.72	16231	2266	5	1	0
Ziprasidone	412.93	116.98	653.96	351.70	319.91	1.554	4.668	−0.08	47.94	16979	2344	5	1	0
Risperidone	410.48	114.65	668.72	364.57	352.73	1.510	2.1	−0.20	57.5	20311	2793	6	0	0

[a] Number of violations from lipinski's rule of five.

interactions with the residues located within the 3 Å region including Phe110, Val111, Asp114, Val115, Leu171, Asn175, Ile183, Ile184, Ala185, Phe189, Trp386, Phe389, Phe390 and Thr412. The binding model of compound **10** displayed well docked ligand in the receptor pocket. The phenylamine nitrogen was involved in hydrogen bonding interaction (3.564 Å) with the NH of His393. The chlorophenyl ring of the molecule was involved in a strong π−π stacking with the phenyl ring of Phe189 and the chloro moiety was involved in hydrophobic interactions with Ile193 and Val190. Good van der Waals interactions were seen with Leu94, Phe110, Val111, Asp114, Val115, Cys118, Glu181, Cys182, Ile 183, Ser 194, Ser197, Trp386, Phe389, Phe390, Tyr408, Ser409, Thr412 and Tyr416 residues located within 3 Å region surrounding the docked molecule.

The phenylamine NH of **11** showed two hydrogen bonding interactions, one each with the backbone nitrogen of Ser194 and OH of Ser193 residue. Further, a π−π stacking interaction was seen between the chlorophenyl ring of the ligand and the phenyl ring of Phe189 similar to **10**. The chloro moiety was engaged in hydrophobic interactions with Ala185, Val190 and His393. Good van der Waals interactions were seen with the vicinity residues (present in 3 Å zone surrounding the docked ligand), namely, Leu94, Phe110, Val111, Asp114, Val115, Cys118, Glu181, Cys182, Ile 183, Val190, Ser194, Ser197, Trp386, Phe389, Phe390, Thr412 and Tyr416. Compound **12** formed a backbone hydrogen bond with carbonyl oxygen of Val111 *via* the indole NH hydrogen. The phenylamine NH was involved in another strong hydrogen bonding interaction with Ala177. Additionally, the chlorophenyl, phenoxy rings were oriented in a way that these yielded a π−cation (4.911 Å) and π−π stacking interactions (3.207 Å) with charged Arg104 and Phe189. The binding was further fortified by very strong van der Waals interactions seen with the proximate residues lying within 3 Å region surrounding the docked molecule including Leu94, Asp114, Val115, Cys118, Leu171, Asn175, Asn176, Asp178, Glu179, Asn180, Glu181, Ile183, Ile184, Ala185, Ser194, Phe389, Phe390 and His393.

The two methoxy derivatives **13** and **14** displayed hydrogen bonding interactions between the indole NH and the backbone nitrogen atom of Trp413. In case of the para methoxy compound **13**, the methoxy oxygen forged another strong hydrogen bond with the OH group of Ser193. The methoxy group was involved in hydrophobic interactions with Phe189, Val190, Ser193. Substantial van der Waals interactions were seen with Leu94, Phe110, Asp114, Val115, Cys118, Cys182, Ile 183, Ser 194, Trp386, Phe389, Phe390, Tyr408, Ser409, Thr412, Trp413 and Tyr416 residues. In compound **14**, the hydrophobic interactions were seen between the methoxy group and Val111, Val115 and Asp175 contributing favorably to the ligand binding in the receptor pocket. The binding energy of the docked molecule was lowered by virtue of strong van der Waals interactions between the docked molecule and proximately placed residues Val91, Leu94, Glu95, Phe110, Asp114, Cys118, Cys182, Ile183, Phe189, Ser193, Ser194, Phe389, Phe390, Tyr408, Ser409, Thr 412 and Tyr416.

Summarizing, the test compounds have shown good affinity towards both 5-HT_{2A} and D_2 receptors comparable to the standard drugs in both the cases suggesting a potential for combined 5-HT_{2A}/D_2 affinity, a profile exhibited by several standard atypical antipsychotic drugs as exemplified by risperidone and ziprasidone. Interestingly, the docking studies showed a different binding mode for the compounds **13** and **14** compared to the rest of the compounds. The ligand−receptor interactions in case of compounds **9** and **12** involved hydrogen bonding to the receptor through the phenylamine system and π−π stacking interaction with the complimentary residues *via* the chlorophenyl system. However, compounds **13** and **14** displayed hydrogen bonding interactions *via* the indole NH and hydrophobic interactions involving the methoxy group. Our receptor binding studies were found to be in

concordance with literature reports. In case of 5-HT_{2A} receptor docking, most of the drugs and test compounds displayed interactions with conserved Asp155 residue as reported earlier [27,28]. Further, multiple binding modes for analogs and binding of same molecule in two alternative modes is an aspect especially highlighted in some previous reports [28]. Similarly, for D_2 receptor binding, the strong and significant interactions with Asp114, Cys118, Phe389 and Phe390were also endorsed by previous literature reports [29].

2.3.2. Computation of physicochemical parameters and ADME profiling

Table 4 lists the values of selected molecular parameters for the compounds **9**–**14** as well as four representative atypical antipsychotic drugs, clozapine, ketanserin, ziprasidone and risperidone. Computation was done employing ChemBio3D Ultra version12.0 after carrying out MM2 minimization of the compound structures. Since, antipsychotics are essentially intended to act on CNS target sites, the blood–brain barrier (BBB) must be crossed for their effect to be exerted. Important molecular descriptors used to predict BBB penetration are molecular surface area parameters (e.g., topological polar surface area TPSA), log P and volume parameters. Further, steric and molecular surface descriptors, e.g., SAS, SEV and ovality and other parameters such as Molecular Topological Index MTI and Weiner Index WI were also calculated. Topological polar surface area, TPSA, which is a recognized parameter for prediction of drug transport properties (in this case, BBB penetration) is a measure of a molecule's hydrogen bonding capacity and its value should not exceed certain limit if the compound is intended to be CNS active. Two differing limits have been proposed: van de Waterbeemd et al. [30] suggest a limit of 90 $A^{\circ 2}$, whereas, Kelder et al. [31] have a lower limit of 60–70 $A^{\circ 2}$. The TPSA values for test compounds were well within these limits (29.66–42.52) which shows that these compounds have a potential to effectively cross the blood brain barrier. ADME prediction methods were used to assess the bioavailability of the active compounds **9**–**14** and the reference drugs. Herein, we calculated the compliance of the prepared compounds to the Lipinski's 'rule of five' which has been widely used as a filter for substances that could likely be further developed in drug design programs. According to this rule, poor absorption or permeation is more likely when there are more than five H-bond donors, ten H-bond acceptors, the molecular weight (MW) is greater than 500 and the calculated Log *P* (CLogP) is greater than 5. Molecules violating more than one of these rules may have problems with bioavailability. Further, TPSA, which is a measure of a molecule's hydrogen bonding capacity, is another key property that has been linked to drug bioavailability. Passively absorbed molecules with a TPSA >140 are thought to have low oral bioavailability [32]. Predictions of ADME properties for studied compounds are given in Table 4. The results show that the synthesized compounds comply with these rules and the standard drugs also do not show any violation. Theoretically, these compounds should present good passive oral absorption and differences in their bioactivity may not be attributed to this aspect.

2.3.3. Computation of blood brain barrier penetration (log BB values)

Several computational methods have been employed for the prediction of blood brain barrier penetration potential of compounds with overall accuracies from 75% to 97%. We assessed our compounds for likely permeation of BBB by calculating their log BB values using an online software program based on topological descriptors [33] (Table 4). The values were also determined for the selection of antipsychotics for comparison. Experimental values of log BB published cover the range from about −2.00 to +1.04. Within this range, compounds with log BB >0.30 cross the BBB readily, while compounds with a log BB< −1.00 are poorly distributed to the brain [34]. The Log BB values for the compounds **9**–**14** (0.38–0.70) were found to be greater than 0.30, suggesting that these have an excellent potential for blood brain barrier penetration.

3. Conclusion

A series of substituted indole derivatives have been synthesized and their preliminary pharmacological evaluation has shown potential atypical antipsychotic effect in chloro substituted compounds **9**, **10**, **11** and **12** and a conventional antipsychotic profile in methoxy based compounds **13** and **14**. Amongst these, compounds **11** and **12** have shown an *in vivo* efficacy superior to the standard drug clozapine. *In silico* (docking studies) carried to investigate the hypothetical binding mode of the target compounds to the dopaminergic D_2 and serotonergic 5-HT_{2A} receptors have suggested a combined D_2/5-HT_{2A} binding profile for the test compounds. Interestingly, the docking studies also showed different binding modes for the compounds displaying typical and atypical profiles in the *in vivo* assays. Further, the compounds comply with Lipinski's rule of five signifying a good absorption and hence, good bioavailability so that the observed differences in bioactivity of the compounds may be attributable to the differences in their chemical structures. The log BB values and TPSA values computed for the test compounds indicate that these have a good potential to penetrate the blood brain barrier and show CNS activity.

4. Experimental protocols

Infrared spectra were recorded in KBr pellets on Perkin Elmer RX 1 spectrophotometer. UV spectra were recorded on Perkin Elmer lambda 15 UV/Visible spectrophotometer. Proton NMR was recorded on Bruker Avance-II, 400 MHz instrument. Proton NMR was recorded on Bruker Avance-II, 400 MHz instrument. For NMR, solutions were made in deuterated chloroform employing tetramethylsilane as internal reference. Mass spectra were obtained with Vg-11-250 J70S spectrometer using electrospray ionization (ESI source). For mass spectra, solutions were made in HPLC grade methanol.

4.1. Synthesis of compounds

4.1.1. Preparation of X-[1-(2-phenylhydrazino)ethyl)phenols (*1*–*2*)

A mixture of 4- or 2-hydroxy acetophenone (12.7 g, 0.092 M) with phenylhydrazine (10.0 g, 0.092 M) was dissolved in 60 ml of ethanol containing a few drops of glacial acetic acid. The mixture was heated on a water bath for 1 h. The reaction mixture was cooled in an ice bath and filtered. The solid obtained was finally washed with water to afford the X-[1-(2-phenylhydrazino)ethyl)phenols.

*4.1.1.1. 4-[1-(2-Phenylhydrazino)ethyl)phenol (**1**).* Yield 91.0%, m.p.168 °C, FTIR (KBr, cm^{-1}): 3449, 3360, 3136, 2960, 1598, 1435, 1499,1365, 1329, 1175,836, 751 and 692. ^1H NMR (400 MHz; $CDCl_3$, δ, *J*): 7.68 (d, 2H, $J = 6.76$ Hz); 7.29–7.23 (m, 3H); 7.17 (d, 2H, $J = 7.52$ Hz); 6.88 (broad s, 1H); 6.86–6.81 (m, 2H); 5.42 (broad s, 1H); 2.19 (s, 3H). MS [ESI, *m*/*z* (relative intensity)]: 227 (83.5) [M + H], 210 (33.00) [*m*/*z* 227 − OH], 209 (17.5) [*m*/*z* 227 − H_2O], 199 (20.4) [*m*/*z* 227 − CO], 184 (20.0) [*m*/*z* 199 −CH_3], 168 (12.5) [*m*/*z* 227 − CH_3–CH(C)OH], 136 (45.3) [OH(C_6H_4)–(C)(NH)CH_3], 133 (100.0) [C_6H_5(NH)–N=(C)CH_3], 119 (21.1) [*m*/*z* 136 −CH_3–H_2].

*4.1.1.2. 2-[1-(2-Phenylhydrazino)ethyl)phenol (**2**).* Yield 87.0%, m.p.141 °C, FTIR (KBr, cm^{-1}): 3450, 3350, 3144, 3055, 1598, 1505,

1498, 1369, 1326, 1129,833, 747 and 691. ^{1}H NMR (400 MHz; $CDCl_3$, δ, J): 12.5 (broad s, 1H); 7.43 (dd, 1H, J = 7.96 Hz, 1.56 Hz); 7.31 (td, 1H, J = 7.00 Hz, 1.92 Hz); 7.22 (td, 2H, J = 7.00 Hz, 1.92 Hz); 7.04 (dd, 2H, J = 7.96 Hz, 1.56 Hz); 7.00 (broad s, 1H); 6.98 (dd, 1H, J = 8.00, 2.00 Hz); 6.94 (td, 1H, J = 7.00 Hz, 1.90 Hz); 6.88 (m, 1H); 2.32 (s, 3H). MS [ESI, m/z (relative intensity)]: 227 (83.5) [M + H], 209 (17.5) [m/z 227 − H_2O], 199 (20.4) [m/z 227 − CO], 184 (20.0) [m/z 199 − CH_3], 136 (40.7) [OH(C_6H_4)–(C)(NH)CH_3], 133 (100.0) [C_6H_5(NH)–N=(C)CH_3].

*4.1.2. Preparation of X-(1H-indol-2-yl)phenols (**3**–**4**)*

4- or 2-hydroxy acetophenone phenylhydrazone (10.0 g, 0.044 M) was heated with 60 g of polyphosphoric acid on an oil bath for 1 h and with continuous stirring maintaining the temperature at 100–120 °C. The mixture was finally poured over crushed ice and stirred well. The precipitates obtained were filtered at the pump and washed well with water affording the corresponding X-(1*H*-indol-2-yl)phenols.

*4.1.2.1. 4-(1H-indol-2-yl)phenol (**3**).* Yield 84.6%, m.p.193–197 °C, FTIR (KBr, cm^{-1}):, 3425, 3212, 3046, 1601, 1498, 1246, 1177, 830 and 749; ^{1}H NMR (400 MHz; $CDCl_3$, δ, J): 9.09 (broad s, 1H); 7.76 (broad s, 1H); 7.58 (d, 2H, J = 7.2 Hz); 7.41 (d, 1H, J = 7.7 Hz); 7.33 (d, 1H, J = 7.9 Hz); 6.91 (m, 1H); 6.82 (d, 2H, J = 7.2 Hz); 6.53 (s, 1H). MS [EI, m/z (relative intensity)]: 211 (17.5) [M + 2], 210 (100.0) [M + H], 192 (3.3) [m/z 210 − H_2O], 182 (5.3) [m/z 210 − CO], 133 (12.3) [m/z 210 − C_6H_4], 116 (8.5) [m/z 210 −C_6H_4–OH].

*4.1.2.2. 2-(1H-indol-2-yl)phenol (**4**).* Yield 92.4%, m.p.187–189 °C. FTIR (KBr, cm^{-1}): 3445, 3349, 3144, 3055, 1590, 1495, 1508, 1370,1324, 1130, 830 and 749; ^{1}H NMR (400 MHz; $CDCl_3$, δ, J): 10.08 (broad s, 1H); 7.90 (broad s, 1H); 7.76 (dd, 1H, J = 7.76 Hz, 1.16 Hz); 7.53 (dd, 1H, J = 7.76 Hz, 1.16 Hz); 7.43 (dd, 1H, J = 7.76 Hz, 1.16 Hz); 7.28 (td, 1H, J = 8.00 Hz, 2.00 Hz); 7.08 (m, 2H); 7.00 (m, 1H); 6.83 (m, 2H). MS [ESI, m/z (relative intensity)]: 210 (100.0) [M + H], 192 (5.3) [m/z 210 − H_2O], 182 (3.7) [m/z 210 − CO], 116 (8.5) [m/z 210 − C_6H_4–OH].

*4.1.3. Preparation of X′-chloro-N-(3-chloropropyl)phenylamines (**5**–**6**)*

A mixture of 4- or 2-chloroaniline (5.0 g, 0.04 M), 1-bromo-3-chloro propane (4.0 ml, 0.04 M) and anhydrous potassium carbonate (5.52 g, 0.04 M) in 70 ml of ethyl methyl ketone was heated under reflux for 8 h. After removal of insoluble solid by filtration, the solvent was evaporated under vacuum yielding X-chloro-*N*-(3-chloropropyl)phenyl amine as a liquid. Yield 5.07 g (62.52%), b.p. 180–183 °C.

*4.1.3.1. 4-Chloro-N-(3-chloropropyl)phenylamines (**5**).* Yield 62.52%, b.p. 180–183 °C. FTIR (KBr, cm^{-1}): 3348, 2921, 1599, 1494, 1302, 1150, 1093, 817, 745 and 675; ^{1}H NMR (400 MHz; $CDCl_3$, δ, J): 7.20 (d, 2H, J = 9.6 Hz); 6.82 (d, 2H, J = 9.6 Hz); 5.75 (broad s, 1H); 3.70 (t, 2H, J = 6.1 Hz); 3.58 (t, 2H, J = 6.1 Hz); 2.25 (q, 2H, J = 6.1 Hz). MS [ESI, m/z (relative intensity)]: 208 (14.2) [M + 4], 206 (69) [M + 2], 204 (100.0) [M + H], 168 (17.3) [m/z 204 − HCl], 154 (5.7) [m/z 204 − $CHCl_3$], 142 (8.8) [ClC_6H_4N=CH_2], 140 (25.1) [ClC_6H_4N=CH_2−2H], 130 (17.2) [m/z 204 − 2HCl], 127 (30.4) [ClC_6H_4NH].

*4.1.3.2. 2-Chloro-N-(3-chloropropyl)phenylamines (**6**).* Yield 77.60%, b.p. 210–212 °C. FTIR (KBr, cm^{-1}): 3342, 2963, 1613, 1491, 1444, 1307, 1152, 1089, 745 and 662; ^{1}H NMR (400 MHz; $CDCl_3$, δ, J): 7.24 (dd, 1H, J = 7.9 Hz, 2.0 Hz); 7.04 (td, 1H, J = 7.3 Hz, 1.8 Hz); 6.75 (dd, 1H, J = 7.9 Hz, 2.0 Hz) 6.68 (td, 1H, J = 7.3 Hz, 1.8 Hz); 3.90 (broad s, 1H); 3.70 (t, 2H, J = 6.1 Hz); 3.53 (t, 2H, J = 6.1 Hz); 2.26 (q, 2H, J = 6.1 Hz). MS [ESI, m/z (relative intensity)]: 208 (6.4) [M + 4], 206 (14.9) [M + 2], 204 (51.3) [M + H], 166 (4.6) [[m/z 204 − HCl] − 2H], 142 (33.9) [ClC_6H_4N=CH_2], 140 (100) [ClC_6H_4N=CH_2] − 2H, 130 (12.4) [m/z 204 − 2HCl], 127 (8.2) [ClC_6H_4NH], 113 (33.8) [ClC_6H_6].

*4.1.4. Preparation of N-(3-chloropropyl)-X′-methoxyphenylamines (**7**–**8**)*

A mixture of 4- or 2-anisidine (5.0 g, 0.04 M), 1-bromo-3-chloro propane (4.0 ml, 0.04 M) and anhydrous potassium carbonate (5.52 g, 0.04 M) in 70 ml of ethyl methyl ketone was heated under reflux for 8 h. After removal of insoluble solid by filtration, the solvent was evaporated under vacuum yielding the corresponding *N*-(3-chloropropyl)-X-methoxyphenylamine products.

*4.1.4.1. N-(3-chloropropyl)-4-methoxyphenylamine (**7**).* Yield 66.9%, b.p. 242–244 °C. FTIR (KBr, cm^{-1}): 3358, 3049, 2980, 1600, 1498, 1436, 1330, 1246, 1170, 1137, 1065, 744 and 690; ^{1}H NMR (400 MHz; $CDCl_3$, δ, J): 8.17 (broad s, 1H); 7.02 (d, 2H, J = 7.2 Hz); 6.72 (d, 2H, J = 7.2 Hz); 3.58 (s, 3H); 3.41 (t, 2H, J = 6.2 Hz); 3.27 (t, 2H, J = 6.2 Hz); 1.83 (q, 2H, J = 6.2 Hz). MS [ESI, m/z (relative intensity)]: 202 (22.9) [M + 2], 200 (63.9) [M + H], 199 (100.0) [M], 164 (9.2) [m/z 200 − HCl], 150 (5.2) [m/z 200 − CH_3Cl], 136 (55.2) [$CH_3OC_6H_4N$=CH_2], 123 (38.6) [$CH_3OC_6H_4$=NH], 108 (19.3) [$CH_3OC_6H_5$].

*4.1.4.2. N-(3-chloropropyl)-2-methoxyphenylamine **(8)**.* Yield 69.3%, b.p. 247–248 °C. FTIR (KBr, cm^{-1}): 3412, 3060, 2937, 1605, 1507, 1457, 1260, 1172, 1118, 1021, 751 and 650; ^{1}H NMR (400 MHz; $CDCl_3$, δ, J): 7.19 (dd, 1H, J = 8.0 Hz, 1.4 Hz); 7.10 (td, 1H, J = 7.8 Hz, 1.4 Hz) 7.00 (td, 1H, J = 7.8 Hz, 1.4 Hz); 6.70 (dd, 1H, J = 8.0 Hz, 1.4 Hz); 4.06 (broad s, 1H); 3.81 (s, 3H); 3.58 (t, 2H, J = 6.6 Hz); 3.30 (t, 2H, J = 6.6 Hz); 2.39 (q, 2H, J = 6.6 Hz). MS [ESI, m/z (relative intensity)]: 202 (20.1) [M+2], 200 (59.4) [M + H], 199 (14.0) [M], 164 (76.6) [m/z 200 − HCl], 150 (4.7) [m/z 200 − CH_3Cl], 136 (100.0) [$CH_3OC_6H_4N$=CH_2], 123 (34.0) [$CH_3OC_6H_4$=NH], 108 (14.3) [$CH_3OC_6H_5$].

Melting point: 247–248 °C. Yield 69.3%.

*4.1.5. Preparation of N-[3-{X-(1H-indol-2-yl)phenoxy}propyl]-X′-chlorophenyl amines (**9**–**12**)*

A mixture of X-(1*H*-indol-2-yl)phenol (**3**–**4**) (5.0 g, 0.024 M) with X′-chloro-*N*-(3-chloropropyl)phenylamines (**5**–**6**) (4.9 g, 0.024 M) and anhydrous potassium carbonate (6.62 g, 0.048 M) in 100 ml of acetone was heated under reflux for 24 h. After removal of insoluble solid by filtration, the solvent was evaporated under vacuum affording the crude *N*-[3-{X-(1*H*-indol-2-yl)phenoxy}propyl]-X′-chlorophenyl amines.

*4.1.5.1. N-[3-{2-(1H-indol-2-yl)phenoxy}propyl]-4-chlorophenylamine (**9**).* Yield 65.83%, m.p. 116–118 °C. UV (λ_{max} (MeOH) 224.6 (ε_{max} 353.22). FTIR (KBr, cm^{-1}): 3349, 2896, 1600, 1450, 1305, 1224, 1090, 1065, 1040 and 745; ^{1}H NMR (400 MHz; $CDCl_3$, δ, J): 9.5 (broad s, 1H); 7.8 (dd, 1H, J = 7.9 Hz, 1.85 Hz); 7.63 (dd, 1H, J = 7.9 Hz, 1.85 Hz) 7.38(dd, 1H, J = 7.9 Hz, 1.85 Hz); 7.30 (td, 1H, J = 7.20 Hz, 1.70 Hz); 7.25 (s, 1H); 7.18 (td, 1H, J = 7.20 Hz, 1.70 Hz); 7.05 (m, 2H); 6.85 (m, 1H); 6.6 (d, 2H, J = 8.8 Hz); 6.5 (d, 2H, J = 8.8 Hz); 4.4 (t, 2H, J = 6.1 Hz); 4.32 (broad s, 1H); 3.75 (t, 2H, J = 6.1 Hz); 2.35 (q, 2H, J = 6.1 Hz). MS [ESI, m/z (relative intensity)]: 379 (13.99) [M + 2], 377 (42.92) [M], 266 (4.88) [$C_6H_4CH(C)NH–C_6H_5O(CH_2)_3NH_2$], 248 (21.95) [$C_6H_4CH(C)NHC_6H_4$ OCH_2 CH=CH_2 − [H], 222 (7.31) [$C_6H_4CH(C)NH$ − C_6H_5O=CH_2], 210 (100) [$C_6H_4CH(C)NH$ C_6H_4 OH], 192 (1.95) [$C_6H_4CH(C)NHC_6H_4$], 168 (21.95) [$ClC_6H_4NHCH_2CH$=CH_2], 152 (9.75) [ClC_6H_4NHCH=CH_2] - [2H], 140 (4.87) [ClC_6H_4N=CH_2], 127 (2.44) [ClC_6H_4NH]. Anal. Calcd. for $C_{23}H_{21}N_2ClO$: C, 73.30; H, 5.62; N, 7.43. Found: C, 73.24; H, 5.59; N, 7.35.

*4.1.5.2. N-[3-{2-(1H-indol-2-yl)phenoxy}propyl]-2-chlorophenylamine (**10**).* Yield 59.55%, m.p. 176–178 °C. UV (λ_{max} (MeOH) 206.2

(ε_{max} = 484.06). FTIR (KBr, cm^{-1}): 3353, 2956, 1610, 1486, 1304, 1233, 1091, 1050, 1030 and 746; ^{1}H NMR (400 MHz; $CDCl_3$, δ, J): 9.6 (broad s, 1H); 7.75 (dd, 1H, J = 7.9, 1.85 Hz); 7.60 (dd, 1H, J = 7.9, 1.85 Hz) 7.35 (dd, 1H, J = 7.9, J = 1.85 Hz); 7.20 (m, 2H); 7.15 (td, 1H, J = 7.20, 1.70 Hz); 7.10 (td, 1H, J = 7.20, 1.70 Hz); 7.00 (m, 3H); 6.85 (m, 1H); 6.70 (dd, 1H, J = 8.1, 1.95 Hz); 6.62 (td, 1H, J = 7.20 Hz, 1.70 Hz); 4.00 (broad s, 1H); 3.65 (t, 2H, J = 6.1 Hz); 3.50 (t, 2H, J = 6.1 Hz); 2.20 (q, 2H, J = 6.1 Hz). MS [ESI, m/z (relative intensity)]: 379 (17.88) [M + 2], 377 (55.89) [M], 264 (9.74) [$C_6H_4CH(C)NH{-}C_6H_5O(CH_2)_3NH_2$] − 2H], 248 (38.46) [$C_6H_4CH(C)NHC_6H_4OCH_2$ CH=CH_2−H], 222 (5.10) [$C_6H_4CH(C)NH{-}C_6H_5O{=}CH_2]^+$, 210 (100) [$C_6H_4CH(C)NHC_6H_4OH$], 192 (15.38) [$C_6H_4CH(C)NHC_6H_4$], 168 (61.53) [$ClC_6H_4NHCH_2CH{=}CH_2$], 152 (6.66) [$ClC_6H_4NHCH{=}CH_2$]−[2H, 140 (5.12) [$ClC_6H_4N{=}CH_2$], 128 (2.44) [$ClC_6H_4NH_2$]. Anal. Calcd. for $C_{23}H_{21}N_2ClO$: C, 73.30; H, 5.62; N, 7.43. Found: C, 73.25; H, 5.79; N, 7.34.

*4.1.5.3. N-[3-{4-(1H-indol-2-yl)phenoxy}propyl]-4-chlorophenylamine (**11**).* Yield 66.30%, m.p. 124–126 °C. UV (λ_{Max} (MeOH) 208.3 (ε_{max} = 259.43). FTIR (KBr, cm^{-1}): 3428, 3051, 2956, 1607, 1455, 1285, 1249, 1182, 1115, 1044 and 747; ^{1}H NMR (400 MHz; $CDCl_3$, δ, J): 7.66 (broad m, 3H); 7.47–7.37 (m, 1H); 7.31 (dd, 1H, J = 7.2, 1.8 Hz); 7.10–7.07 (m, 4H); 6.89 (d, 2H, J = 8.4 Hz); 6.80 (s, 1H); 6.57 (d, 2H, J = 8.4 Hz); 3.53 (t, 2H, J = 6.6 Hz); 3.26 (t, 2H, J = 6.6 Hz); 3.30 (broad s, 1H); 2.08 (q, 2H, J = 6.6 Hz). MS [ESI, m/z (relative intensity)]: 379 (3.8) [M + 2], 377 (17.8)[M], 340 (6.6) [M − HCl], 338 (100) [M − HCl−2H], 286 (91.1) [m/z 340 − C_4H_4], 248 (44.3) [$C_6H_4CH(C)NHC_6H_4OCH_2CH{=}CH_2$−H], 220 (74.7) [$C_6H_4CH(C)NH{-}C_6H_5O{=}CH_2{-}H_2$], 210 (52.7) [$C_6H_4CH(C)NHC_6H_4OH$], 192 (11.0) [$C_6H_4CH(C)NHC_6H_4$]. Anal. Calcd. for $C_{23}H_{21}N_2ClO$: C, 73.30; H, 5.62; N, 7.43. Found: C, 73.40; H, 5.52; N, 7.26.

*4.1.5.4. N-[3-{4-(1H-indol-2-yl)phenoxy}propyl]-2-chlorophenylamine (**12**).* Yield 61.50%, m.p. 153–155 °C. UV (λ_{Max} (MeOH) 208.2 (ε_{max} = 424.56). FTIR (KBr, cm^{-1}): 3422, 3065, 2957, 1598, 1509, 1459, 1289, 1175, 1094, 1034 and 744; ^{1}H NMR (400 MHz; $CDCl_3$, δ, J): 8.32 (broad s, 1H); 7.60 (d, 2H, J = 8.7 Hz); 7.26 (dd, 2H, J = 7.8, 1.5 Hz); 7.14 (m, 2H); 6.98 (d, 2H, J = 8.7 Hz); 6.71(dd, 1H, J = 8.4, J = 1.4 Hz); 6.70 (dd, 1H, J = 8.4 Hz, 1.2 Hz); 6.63 (m, 2H); 6.55 (s, 1H); 4.16 (broad s, 1H); 3.66 (t, 2H, J = 6.6Hz); 3.40 (t, 2H, J = 6.6 Hz); 2.10 (q, 2H, J = 6.6 Hz). MS [ESI, m/z (relative intensity)]: 379 (4.4) [M + 2], 377 (10.3) [M − HCl], 286 (3.2) [m/z 340 − C_4H_4], 247 (12.7) [$C_6H_4CH(C)NH\ C_6H_4OCH_2CH{=}CH_2$−2H], 234 (10.5) [M − $ClC_6H_4NH_2{-}CH_3$], 222 (100.0) [C_6H_4CH (C)NH−$C_6H_5O{=}CH_2{-}H_2$], 220 (17.2) [$C_6H_4CH(C)NH{-}C_6H_5O{=}CH_2{-}H_2$], 210 (100) [$C_6H_4CH(C)NHC_6H_4OH$], 168 (9.4) [$ClC_6H_4NHCH_2CH{=}CH_2$], 140 (18.2) [$ClC_6H_4$ N=CH_2], 127 (4.6) [ClC_6H_4NH]. Anal. Calcd. for $C_{23}H_{21}N_2ClO$: C, 73.30; H, 5.62; N, 7.43. Found: C, 73.14; H, 5.59; N, 7.39.

*4.1.6. Preparation of N-[3-{X-(1H-indol-2-yl)phenoxy}propyl]-X′-methoxyphenyl amines (**13**–**14**)*

A mixture of 4-(1*H*-indol-2-yl)phenol (**3**) (4.1 g, 0.02 M), *N*-(3-chloropropyl)-X′-methoxyphenylamines (**7**–**8**) (4.0 g, 0.02 M) and anhydrous potassium carbonate (5.5 g, 0.04 M) in 100 ml of acetone was heated under reflux for 24 h. After removal of insoluble solid by filtration, the solvent was evaporated under vacuum affording the crude compounds which were subsequently recrystallized from ethanol.

*4.1.6.1. N-[3-{4-(1H-indol-2-yl)phenoxy}propyl]-4-methoxyphenylamine (**13**).* Yield 60.56%, m.p. 200–202 °C. UV (λ_{Max} (MeOH) 207.0 (ε_{max} = 427.91). FTIR (KBr, cm^{-1}): 3419, 3049, 2912, 1605, 1503, 1454, 1280, 1257, 1080, 986 and 748; ^{1}H NMR (400 MHz; $CDCl_3$, δ, J): 8.38 (broad s, 1H); 7.65 (d, 2H, J = 9.0 Hz); 7.60 (d, 2H, J = 8.0 Hz); 7.37 (d, 2H, J = 9.0 Hz); 7.16–7.09 (m, 2H); 6.99 (d, 2H, J = 9.0 Hz); 6.95 (m, 1H); 6.85 (m, 1H); 6.71 (s, 1H); 4.16 (t, 2H, J = 6.2 Hz); 3.84 (s, 3H); 3.76 (t, 2H, J = 6.2 Hz); 3.48 (broad s, 1H); 2.26 (q, 2H, J = 6.2 Hz). MS [ESI, m/z (relative intensity)]: 373 (30.8) [M + H], 214 (11.6) [m/z 266−C_4H_4], 212 (34.1) [m/z 214 − 2H], 210 (19.5) [$C_6H_4CH(C)NHC_6H_4OH$], 192 (44.7) [$C_6H_4CH(C)NHC_6H_4$], 164 (28.3) [$CH_3OC_6H_4NHCH_2CH{=}CH_2$], 150 (20.2) [$CH_3OC_6H_4NHCH{=}CH_2$], 136 (100) [$H_3CO(C_6H_4)N{=}CH_2$], 123 (91.4)[$CH_3OC_6H_4{=}NH$], 108 (59.2) [$CH_3OC_6H_5$]. Anal. Calcd. for $C_{24}H_{24}N_2O_2$: C, 77.39; H, 6.49; N, 7.52. Found: C, 77.29; H, 6.32; N, 7.40.

*4.1.6.2. N-[3-{4-(1H-indol-2-yl)phenoxy}propyl]-2-methoxyphenylamine (**14**).* Yield 64.2%, m.p. 216–218 °C. UV (λ_{Max} (MeOH) 208.2 (ε_{max} = 558.14). FTIR (KBr, cm^{-1}): 3428, 3141, 2938, 1604, 1454, 1280, 1251, 1116, 1025 and 747; ^{1}H NMR (400 MHz; $CDCl_3$, δ, J): 8.72 (broad s, 1H); 7.61 (d, 2H, J = 6.8 Hz); 7.58 (m, 1H); 7.40 (d, 1H, J = 8.0 Hz); 7.14 (td, 1H, J = 7.2 Hz, 1.7 Hz); 7.08 (td, 1H, J = 7.2 Hz, 1.7 Hz); 6.94 (m, 3H); 6.90-6.88 (m, 2H); 6.81 (m, 1H); 6.70 (s, 1H, J = 1.4 Hz); 4.15 (t, 2H, J = 6.2 Hz); 3.92 (s, 3H); 3.76 (t, 2H, J = 6.2 Hz); 3.05 (broad s, 1H); 2.34 (q, 2H, J = 6.2 Hz). MS [ESI, m/z (relative intensity)]: 373 (28.9) [M + H], 266 (2.8) [$C_6H_4CH(C)NH{-}C_6H_5O(CH_2)_3NH_2$], 214 (10.6) [$m/z$ 266 − C_4H_4], 212 (28.9) [m/z 214 − 2H], 210 (21.0) [$C_6H_4CH(C)NHC_6H_4OH$], 192 (1.2) [$C_6H_4CH(C)NHC_6H_4$], 164 (39.2) [$CH_3OC_6H_4NHCH_2CH{=}CH_2$], 150 (13.0) [$CH_3OC_6H_4NHCH{=}CH_2$], 136 (100) [$H_3CO(C_6H_4)N{=}CH_2$], 123 (88.0) [$CH_3OC_6H_4{=}NH$], 108 (37.7) [$CH_3OC_6H_5$]. Anal. Calcd. for $C_{24}H_{24}N_2O_2$: C, 77.39; H, 6.49; N, 7.52. Found: C, 77.22; H, 6.29; N, 7.45.

4.2. Preliminary pharmacological evaluation for atypical antipsychotic effect

4.2.1. Apomorphine induced mesh climbing assay

Albino lyka mice (5 mice in each group) of either sex (26–38 g) were habituated by individually placing in a circular cage made of wire mesh of diameter 13 cm and height 14 cm. Mice in the test groups were injected with the test compound intraperitoneally and returned to the home cage. Mice in the control groups were injected with normal saline intraperitoneally and returned to the home cage. Mice in the clozapine test groups were injected with clozapine intraperitoneally and returned to the home cage. After a gap of 10 min, apomorphine (2.5 mg/kg) was injected intraperitoneally. Mesh climbing behavior was noted for the naïve or untreated group at the start and then, readings were noted at 10, 15, 20, 25 and 30 min after the apomorphine injection by placing the mice in the mesh cage for 60 s. Severity of the climbing behavior was scored as: 1 (one, two or three paws on the mesh) and 2 (all four paws on the mesh).

4.2.2. Apomorphine induced stereotypy assay

The same albino lyka mice employed in the mesh climbing assay were used. Each mouse was injected with either the vehicle or the test compound or clozapine and returned to its home cage. After a gap of 10 min, apomorphine (2.5 mg/kg) was injected. Stereotypy was noted similarly at 10, 15, 20, 25 and 30 min after apomorphine injection by placing the animal in an inverted 500 ml beaker for 60 s. Scoring of stereotypy was done as: 1 (rearing, sniffing, grooming) and 2 (licking, biting). Three dose levels were employed and doses were selected by initial titration at different dose levels. The atypical antipsychotic drug clozapine was employed as a separate group (positive control) for comparison.

4.3. Docking studies

The computational studies were carried out using Dell notebook PC, (Core 2 Duo Processor; 4GB RAM) running on Windows 7 using Maestro 9.3. The synthesized molecules were evaluated *in silico*

(docking) using the homology models of serotonergic 5-HT_{2A} and dopamine D_2 receptors. Various parameters including docking score, glide score and glide emodel were calculated. Similar data emphasizing the degree of interaction between the test compounds and receptor were deduced additionally.

4.3.1. Selection of the protein

4.3.1.1. Serotonin 5-HT_{2A} receptor structure. The model of serotonergic 5-HT_{2A} receptor employed for the *in silico* evaluation was retrieved from ModBase. Initially, the Swiss-Prot data base was screened for the dopamine D_2 receptor and the most relevant model (UniProt ID: P28233) was selected. Swiss-Prot is the manually annotated and reviewed section of the UniProt KnowledgeBase (UniProtKB). Finally, the comparative models for this Swiss-Prot ID were screened. The selected model was based on template of thermo-stabilized, *N*-ethyl-5′-carboxamido adenosine bound human A_{2A} receptor (PDB ID: 2ydvA), whose structure was determined at 2.60Å. The model contained 324 amino acid residues, ranging from residue numbers 84–407. The model was selected based on the notified reliability criteria and chain length.

4.3.1.2. Dopamine D_2 receptor structure. The model of the dopaminergic D_2 receptors employed for the *in silico* evaluation was obtained from ModBase by initial screening of the Swiss-Prot data base (UniProt ID: P14416) was selected. The model selected was based on human β_2-adrenergic receptor template (PDB ID: 2RH1), whose crystal structure was determined at 2.40 Å. The model contains net 414 residues, ranging from amino acids 30 to 442. The model was selected based on the notified reliability criteria and chain length.

4.3.2. Preparation of protein

The pre-processing of the protein was carried out by assigning the bond orders, adding hydrogen atoms to the crystal structure, creating disulfide bonds, filling missing side chains and loops (using Prime). The water molecules beyond 5 Å were deleted straightaway. This was followed by reviewing and modifying the pre-processed protein, where the workspace protein was analyzed for multiple chains and associated ligands. In the next step (refinement), hydrogen bonds were optimized using PROPKA at pH of 7. The amino acids residues lying close to the active site were allowed to flip. Finally, the strain was minimized using OPLS2005. The quality of prepared protein was ascertained by Ramachandran plot.

4.3.3. Receptor grid generation

4.3.3.1. Serotonin 5-HT_{2A} receptor. The receptor grid for docking was prepared by Receptor Grid generation tool, under glide menu. The receptor was defined by default settings as the workspace structure. The van der Waals radii were scaled by a factor of 1.0 for all those atoms carrying partial atomic charge. As suggested in literature, the receptor grid site was selected as the centroid of residues Asp120 and Asp155. No constraints and excluded volumes were added. The default settings were applied for grid generation.

4.3.3.2. Dopamine D_2 receptor. In the Receptor Grid generation wizard, the receptor was defined by default settings as the workspace structure. The van der Waals radii were scaled by a factor of 1.0 for all those atoms carrying partial atomic charge. As suggested in literature, the receptor grid site was selected as the centroid of residues Asp114, Ser193 and Phe390. No constraints and excluded volumes were defined. The grid was generated retaining the default settings; dock ligands with less than 20 Å length and the diameter midpoint of each docked ligand was required to remain within a cube of edge length of 10 Å whose centroid overlapped with the centroid of mentioned residues.

4.3.4. Ligand preparation

All ligand 2D structures were sketched in ChemDraw Ultra12.0 and were saved as .sdf files and then imported to Maestro 9.3. The ligands were selected as entries and were subjected to minimization using the OPLS_2005 force field and various ionization states between pH 7 ± 2 were generated. The prepared ligands were saved in maestro format. The operation was performed under the LigPrep wizard.

4.3.5. Ligand docking

Various conformations of the ligands generated by LigPrep were docked employing Ligand Docking tool under the Glide menu. The receptor grid and ligands were defined by browsing the respective files. Docking was performed using extra precision mode with generation of at most 10 poses per ligand. Besides, per residue interaction scores were also calculated during the run. Docking efficiency was evaluated on the basis of various parameters including Docking score, GScore, Glide emodel, potential energy, binding energy and complex energy.

Acknowledgments

The research grant provided by the University Grants Commission is duly acknowledged.

References

[1] S. Saha, D. Chant, J. Welham, J. McGrath, A systematic review of the prevalence of schizophrenia, PLoS Med. 2 (2005) 141.
[2] M.D. Jibson, I.D. Glick, R. Tandon, Schizophrenia and other psychotic disorders, Focus 2 (2004) 17–30.
[3] J.M. Stone, P.D. Morrison, L.S. Pilowsky, Glutamate and dopamine dysregulation in schizophrenia – a synthesis and selective review, J. Psychopharmacol. 21 (2007) 440–452.
[4] B. Knutson, S.E. Gibbs, Linking nucleus accumbens dopamine and blood oxygenation, Psychopharmacology (Berlin) 191 (2007) 813–822.
[5] P. Seeman, Targeting the dopamine D_2 receptor in schizophrenia, Expert Opin. Ther. Targets 10 (2006) 515–531.
[6] K. Melkersson, M.L. Dahl, Adverse metabolic effects associated with atypical antipsychotics: literature review and clinical implications, Drugs 64 (2004) 701–723.
[7] R.R. Conley, D.L. Kelly, Second-generation antipsychotics for schizophrenia: a review of clinical pharmacology and medication-associated side effects, Isr. J. Psychiatry Relat. Sci. 42 (2005) 51–56.
[8] J.W. Newcomer, Metabolic considerations in the use of antipsychotic medications: a review of recent evidence, J. Clin. Psychiatry 68 (1) (2007) 20–27.
[9] G. Kerti, T. Kurtán, K.E. Kövér, S. Sólyom, I. Greiner, S. Antus, Synthesis and circular dichroism of optically active 1,3-disubstituted isochromans of dopamine D_4 antagonist activity, Tetrahedron Asymm. 21 (2010) 2356–2360.
[10] R. Ortega, H. Hübner, P. Gmeiner, C.F. Masaguer, Aromatic ring functionalization of benzolactam derivatives: new potent dopamine D_3 receptor ligands, Bioorg. Med. Chem. Lett. 21 (2011) 2670–2674.
[11] M. Tomic, D. Ignjatovic, G. Tovilovic, D. Andric, G. Roglic, S. Kostic-Rajacic, Two new phenylpiperazines with atypical antipsychotic potential, Bioorg. Med. Chem. Lett. 17 (2007) 5749–5753.
[12] J.M. Graham, L.L. Coughenour, B.M. Barr, D.L. Rock, S.S. Nikam, 1-Aminoindanes as novel motif with potential atypical antipsychotic properties, Bioorg. Med. Chem. Lett. 18 (2008) 489–493.
[13] A. Loevezijn, J. Venhorst, W.I.I. Bakker, V. de Looff, S. Verhoog, *N*-(Arylsulfonyl) pyrazoline-1-carboxamidines as novel, neutral 5-hydroxytryptamine6 receptor (5-HT_6R) antagonists with unique structural features, J. Med. Chem. 54 (2011) 7030–7054.
[14] M.L. Lolli, S.L. Hansen, B. Rolando, B. Nielsen, P. Wellendorph, K. Madsen, O.M. Larsen, U. Kristiansen, R. Fruttero, A. Gasco, T.N. Johansen, Hydroxy-1,2,5-oxadiazolyl moiety as bioisoster of the carboxy function: synthesis, ionization constants and pharmacological characterization of γ-aminobutyric acid (GABA) related compounds, J. Med. Chem. 49 (2006) 4442–4446.
[15] M. Leopoldo, E. Lacivita, P.D. Giorgio, C. Fracasso, S. Guzzetti, S. Caccia, M. Contino, A.N. Colabufo, F. Berardi, R. Perrone, Structural modifications of *N*-(1,2,3,4,-tetrahydronaphthalen-1-yl)-4-aryl-1-piperazinehexanamides: influence on lipophilicity and 5-HT_7 receptor activity. Part III, J. Med. Chem. 51 (2008) 5813–5822.
[16] S. Butini, S. Gemma, G. Campiani, S. Franceschini, F. Trotta, M. Borriello, N. Ceres, S. Ros, S.S. Coccone, M. Bernetti, M. De Angelis, M. Brindisi, V. Nacci, I. Fiorini, E. Novellino, A. Cagnotto, T. Mennini, K. Sandager-Nielsen,

J.T. Andreasen, J. Scheel-Kruger, J.D. Mikkelsen, C. Fattorusso, Discovery of a new class of potential multifunctional atypical antipsychotic agents targeting dopamine D3 and serotonin 5-HT1A and 5-HT2A receptors: design, synthesis, and effects on behavior, J. Med. Chem. 52 (2009) 151–169.
[17] Y. Chen, X. Xu, X. Liu, B. Liu, G. Zhang, Synthesis and evaluation of a series of 2-substituted-5-thiopropylpiperazine (piperidine)-1,3,4-oxadiazoles derivatives as multireceptor atypical antipsychotics, PLoS One 7 (2012) e35186.
[18] Y. Chen, S. Wang, X. Xu, M. Yu, S. Liu, X. Liu, B. Liu, G. Zhang, Synthesis and biological investigation of a series of coumarin piperazine (piperidine) derivatives as potential atypical antipsychotics, J. Med. Chem. 56 (2013) 4671–4690.
[19] Y. Chen, X. Xu, X. Liu, B. Liu, G. Zhang, Synthesis and evaluation of a series of piperidine-2,6-dione-piperazine (piperidine) derivatives as multireceptor atypical antipsychotics, Arch. Pharm. Chem. Life Sci. 345 (2012) 859–869.
[20] H.G. Vogel (Ed.), Drug Discovery and Evaluation: Pharmacological Assays, third ed., Springer, New York, 2007, pp. 761–762.
[21] A. Bali, S. Malhotra, H. Dhir, A. Kumar, A. Sharma, Synthesis and evaluation of 1-(quinoliloxypropyl)-4-aryl piperazines for atypical antipsychotic effect, Bioorg. Med. Chem. Lett. 19 (2009) 3041–3044.
[22] A. Bali, K. Sharma, A. Bhalla, S. Bala, D. Reddy, A. Singh, A. Kumar, Synthesis, evaluation and computational studies on a series of acetophenone based 1-(aryloxypropyl)-4-(chloroaryl) piperazines as potential atypical antipsychotics, Eur. J. Med. Chem. 45 (2010) 2656–2662.
[23] A. Bali, A.C.D.K. Reddy, Synthesis and evaluation of *meta* substituted 1-(aryloxypropyl)-4-(chloroaryl) piperazines as potential atypical antipsychotics, Med. Chem. Res. 22 (2013) 382–391.
[24] E. Fischer, O. Hess, Synthese von indolderivaten, Ber. Dtsch. Chem. Ges 17 (1884) 559–568.
[25] http://www.uniprot.org/uniprot/P28223.
[26] http://www.uniprot.org/uniprot/P14416.
[27] S.P. Runyon, P.D. Mosier, B.L. Roth, R.A. Glennon, R.B. Westkaemper, Potential modes of interaction of 9-aminomethyl-9,10-dihydroanthracene (AMDA) derivatives with the 5-HT_{2A} receptor: a ligand structure-affinity relationship, receptor mutagenesis and receptor modeling investigation, J. Med. Chem. 51 (2008) 6808–6828.
[28] C. Dezi, J. Brea, M. Alvarado, E. Ravina, C.F. Masaguer, M.I. Loza, F. Sanz, M. Pastor, Multistructure 3D-QSAR studies on a series of conformationally constrained butyrophenones docked into a new homology model of the 5-HT_{2A} receptor, J. Med. Chem. 50 (2007) 3242–3255.
[29] R. Aranda, K. Villalba, E. Ravina, C.F. Masaguer, J. Brea, F. Areias, E. Domınguez, J. Selent, L. Lopez, F. Sanz, M. Pastor, Synthesis, binding affinity and molecular docking analysis of new benzofuranone derivatives as potential antipsychotics, J. Med. Chem. 51 (2008) 6085–6094.
[30] H. van de Waterbeemd, G. Camenisch, G. Folkers, J.R. Chretien, O.A. Raevsky, Estimation of blood-brain barrier crossing of drugs using molecular size and shape and H-bonding descriptors, J. Drug Target. 6 (1998) 151–165.
[31] J. Kelder, P.D.J. Grootenhuis, D.M. Bayada, L.P.C. Delbressine, J.P. Ploemen, Polar molecular surface as a dominating determinant for oral absorption and brain penetration of drugs, Pharm. Res. 16 (1999) 1514–1519.
[32] D.E. Clark, S.D. Pickett, Computational methods for the prediction of "drug-likeness", Drug Discov. Today 5 (2000) 49–58.
[33] http://www.chemsilico.com/CS_prBBB/BBBhome.html.
[34] M. Iyer, R. Mishra, Y. Han, A. Hopfinger, Predicting blood-brain partitioning of organic drugs using membrane-interaction QSAR analysis, J. Pharm. Res. 19 (2002) 1611–1621.